Size Determination of Cyanobacterial and Higher Plant Photosystem II by Gel Permeation Chromatography, Light Scattering, and Ultracentrifugation†

Athina Zouni,*,‡ Jan Kern,‡ Joachim Frank,‡ Thomas Hellweg,§ Joachim Behlke,|| Wolfram Saenger,⊥ and Klaus-Dieter Irrgang*,‡

Max-Volmer-Laboratorium, Technische Universität Berlin, Strasse des 17. Juni 135, D-10623 Berlin, Germany, Iwan-N.-Stranski-Laboratorium, Technische Universität Berlin, Strasse des 17. Juni 122, D-10623 Berlin, Germany, Max-Delbrück-Centrum für Molekulare Medizin Berlin Buch, Robert-Rössle-Strasse 10, D-13092 Berlin, Germany, and Institut für Kristallographie, Freie Universität Berlin, Takustrasse 6, D-14195 Berlin, Germany

Received October 29, 2004; Revised Manuscript Received December 21, 2004

ABSTRACT: The oxygen-evolving photosystem II core complexes (PSIIcc) from the thermophilic cyanobacterium *Thermosynechococcus elongatus* (PSIIcc*Te*) and the higher plant *Spinacia oleracea* (PSIIcc*So*) have been isolated from the thylakoid membrane by solubilization with *n*-dodecyl-*β*-D-maltoside, purified and characterized by gel permeation chromatography (GPC), dynamic light scattering (DLS), and analytical ultracentrifugation (AUC). DLS suggests that PSIIcc from both organisms exists as a monomer in dilute solution and aggregates with increasing protein concentration. In contrast to DLS, GPC and AUC showed that PSIIcc of both organisms occur as monomers and dimers, and it became clear from our studies that calibration of GPC columns with soluble proteins leads to wrong estimates of the molecular masses of membrane proteins. At a PSIIcc protein concentration of 0.2 mg/mL, molar masses, *M*, of 756 ± 18 kDa and 710 ± 15 kDa for dimeric PSIIcc*Te* and PSIIcc*So*, respectively, were determined by analytical ultracentrifugation. At very low protein concentrations, at or below 0.05 mg/mL, the dimeric form of PSIIcc*Te* partially dissociates (20−30%) to form monomers. On the basis of these studies 3-dimensional crystals of PSIIcc*Te* were obtained that contain dimers in the asymmetric unit [Zouni, A. et al. (2001) *Nature 409*, 739−743]. Using synchrotron radiation the crystals diffract to a resolution of 3.8 Å, which has been improved recently to 3.2 Å [Biesiadka, J., et al. (2004) *Phys. Chem. Chem. Phys. 6*, 4733−4736].

In plants, green algae, and cyanobacteria, oxygenic photosynthesis is catalyzed by two chlorophyll-containing protein complexes, photosystems I and II (PSI, PSII),[1] which are connected in series. They are located in the thylakoid membrane and utilize light energy to oxidize water. This process is initiated by light captured by chlorophyll *a* (Chl*a*) in antenna proteins and channeled to the primary donor P680 of PSII located near the luminal side of the reaction center (RC). The RC is formed by a pair of Chl*a* molecules called P680 or by four Chl*a* molecules (P_{D1}, P_{D2}, Chl_{D1}, Chl_{D2}) according to the multimer model (*1*, *2*) which are coordinated to the membrane-embedded protein subunits D1 and D2. During charge separation in the RC, an electron is transferred to the stromal side along a sequence of electron acceptors comprising a Chl*a*, a pheophytin, and two plastoquinones Q_A and Q_B, coupled by a non-heme iron. At the oxidizing site of PSII, a redox active tyrosine residue Tyr_Z reduces $P680^{+\bullet}$ and the oxidized Tyr_Z withdraws electrons from a tetrameric Mn-cluster on the luminal side of the thylakoid membrane, which in turn oxidizes water molecules, leading to the release of protons, electrons, and molecular oxygen (*3*, *4*). The electrons released by PSII via doubly reduced Q_B are transferred to PSI and from there via water-soluble ferredoxin to $NADP^+$-reductase to produce the strongly reducing NADPH. The released protons form a pH gradient over the thylakoid membrane that is required by ATP synthetase to form ATP. Finally, both ATP and NADPH reduce CO_2 to carbohydrates in the Calvin cycle that create biomass, food, and fuel (*5*).

During isolation of PSII from the thermophilic cyanobacterium *Thermosynechococcus elongatus (T. elongatus)*, the extrinsic antenna system formed by the phycobilisomes is lost and contaminating PSI and ATP synthase are removed (*6*). This PSII core complex (PSIIcc) is functionally active and consists of at least 19 membrane intrinsic and extrinsic

† This work was supported by DFG-Sonderforschungsbereich 498 (TP C7, A4) and by Fonds der Chemischen Industrie (Frankfurt/Main, Germany) in cooperation with the Bundesministerium für Bildung und Forschung (BMBF, Bonn, Germany).

* Corresponding authors. A.Z.: phone, +49-30-31425580; fax, +49-30/314 21122; e-mail, Zouni@phosis1.chem.tu-berlin.de. K.-D.I.: phone, +49-30-31422713; fax, +49-30/31421122; e-mail, Irrg0532@mailbox.tu-berlin.de.

‡ Max-Volmer-Laboratorium, Technische Universität Berlin.

§ Iwan-N.-Stranski-Laboratorium, Technische Universität Berlin.

|| Max-Delbrück-Centrum für Molekulare Medizin Berlin Buch.

⊥ Freie Universität Berlin.

[1] Abbreviations: AUC, analytical ultracentrifugation; Chl*a*, chlorophyll *a*; DLS, dynamic light scattering; *β*-DM, *n*-dodecyl-*β*-D-maltoside; FPLC, fast protein liquid chromatography; GPC, gel permeation chromatography; HPLC, high performance liquid chromatography; *M*, molar mass; PEG, polyethylene glycol; PS, photosystem; PSIIcc, photosystem II core complex; PSIIcc*Te*, photosystem II core complex from *Thermosynechococcus elongatus*; PSIIcc*So*, photosystem II core complex from *Spinacia oleracea*; PSI*Te*, photosystem I from *Thermosynechococcus elongatus*; R_H, hydrodynamic radius.

10.1021/bi047685q CCC: $30.25
Published on Web 02/25/2005

proteins. Besides the two RC proteins D1 and D2 (*7*, *8*) the core complex contains two antenna proteins known as CP47 (*psbB* gene product) and CP43 (*psbC* gene product), which contain about 30 Chl*a* and 8−10 carotenoid molecules. Cytochrome *b559* is formed by subunits α (5 kDa) and *β* (9 kDa) (*psbE* and *psbF* gene products). These intrinsic membrane protein components are also found in PSIIcc from higher plants such as *Spinacia oleracea*. In cyanobacterial PSIIcc three extrinsic proteins are associated at the luminal side: the 33 kDa protein (*psbO* gene product), a 12 kDa protein (*psbU* gene product), and a cytochrome *c550* with a molecular mass of 17 kDa (*psbV* gene product). Of these proteins, only the 33 kDa protein is found in *S. oleracea* PSIIcc (PSIIcc*So*), while the other two are replaced by 23 kDa (*psbP*) and 16 kDa (*psbQ*) proteins, respectively (*9*). In addition to these 9 proteins, the PSIIcc of both *T. elongatus* (PSIIcc*Te*) and *S. oleracea* (PSIIcc*So*) contain at least 10 smaller subunits in the range ≤10 kDa (*10*) of mostly unknown function (*11*).

Concerning the molecular mass of PSIIcc (the oligomerized state of PSII) from both cyanobacteria and higher plants, there are two conflicting proposals in the literature. In one, PSIIcc exists as a monomer with an effective molecular mass of 318 ± 50 kDa (*12*−*17*). In the other, PSIIcc occurs as a dimer (*18*−*26*) with an effective molecular mass in the range between 450 kDa (*13*) and 812 kDa (*19*). This molecular mass range was determined by gel permeation chromatography (GPC) and electron microscopy image analysis and depends on the preparation conditions, for example the detergent used (*27*, *28*), and on the methods employed in these studies.

The work presented here was initiated to obtain well-characterized samples of PSIIcc*Te* and of PSIIcc*So* for crystallization experiments. The two functionally active fractions of PSIIcc*Te* separated by anion exchange chromatography (*6*) probably represent monomeric and dimeric PSIIcc*Te* in solution. For PSIIcc*So* isolated by sucrose density gradients, an upper and a lower band were observed (previously designated as PSIIcc and PSIIcc*), which may contain monomeric and dimeric PSIIcc*So* (*12*, *29*). Because the aggregation state is crucial for the design of crystallization experiments, we studied the aggregation behavior of both fractions I and II of PSIIcc*Te* and the upper and lower bands of PSIIcc*So*. GPC, dynamic light scattering (DLS), and analytical ultracentrifugation (AUC) indicated that PSIIcc from the two organisms had different aggregation behavior in solution. The results are discussed from a crystallization point of view.

MATERIALS AND METHODS

All chemicals used in the present work were of analytical grade. Water was deionized through a Millipore-Q device. The following buffers were used for measurements: buffer A, 20 mM MES−NaOH, pH 6.0, 0.02% *β*-DM, 20 mM $CaCl_2$, 25 mM $MgSO_4$, 5% glycerol; buffer B, 25 mM MES−NaOH, pH 6.5, 10 mM $CaCl_2$, 0.025% *β*-DM, 35% w/v sucrose; buffer C, 5 mM MES−NaOH, pH 6.4, 0.02% *β*-DM, 50 mM $MgSO_4$.

Protein Purification. The oxygen-evolving PSIIcc*Te* was extracted from thylakoid membranes of *T. elongatus* (*30*), purified, and separated into two fractions by anion exchange chromatography (hereafter designated as fraction I and fraction II) (*6*). Fraction I (monomeric PSIIcc*Te*) and fraction II (dimeric PSIIcc*Te*) show oxygen evolution rates at saturating light between 1700 and 3000 *μ*mol of O_2 (mg Chl h)$^{-1}$ and 2200−3700 *μ*mol of O_2 (mg Chl h)$^{-1}$, respectively (6). Single flash yields for monomeric and dimeric PSIIcc*Te* were reported to be between 38-69 (1/4 O_2 flash)$^{-1}$ and 37−73 (1/4 O_2 flash)$^{-1}$, repectively (6). PSIIcc from *Spinacia oleracea* was isolated as upper and lower bands of sucrose density gradient centrifugation (*12*, *29*). Lower band PSIIcc*So* showed average oxygen evolution rates of 1400 ± 30 *μ*mol of O_2 (mg Chl h)$^{-1}$ and maximum values of 1800 ± 100 *μ*mol of O_2 (mg Chl h)$^{-1}$ and upper band PSIIcc*So* 750−850 *μ*mol of O_2 (mg Chl h)$^{-1}$. We have also analyzed the number of Chls per oxygen evolving center by measuring at the flash light induced O_2 release patterns as described in ref *29*. The following values were obtained: on the average 70 Chl and minimally 60 ± 5 Chl per oxygen center for lower band PSIIcc*So* and for upper band PSIIcc*So* 120 ± 20 Chl. Photochemical activities were determined by measuring the turnover of the primary plastoquinone acceptor Q_A at 325 nm as described in (*6*) yielding 45 ± 5 Chl/per Q_A for lower band PSIIcc*So*, 70 ± 5 for upper band PSIIcc*So*.

Trimeric PSI from *T. elongatus* (PSI*Te*) was purified as described (*31*), and monomeric PSI was obtained from trimeric PSI by osmotic shock treatment as described in ref *32*.

Isolation and purification of CP29 from spinach chloroplasts followed a modification of the protocol reported in ref *33* as described in ref *34*. CP47 and LHC II were isolated and purified from spinach PSII according to ref *35* and as described in refs *36* and *37*.

Determination of the Protein and Chlorophyll Concentrations. Absorbance spectra were recorded at room temperature using a Shimadzu UV 3000 spectrophotometer with an optical path length of 1 cm. Chl*a* concentrations were determined after extraction with 80% acetone (*38*). The protein concentrations of PSIIcc*Te* and PSIIcc*So* were calculated by assuming that 36 and 40 Chl*a* are bound per P680, respectively (*28*, *39*, *40*). PSI*Te* concentration was calculated by assuming that 96 Chl*a* are bound per primary donor P700 (*41*). In addition protein concentrations were determined using bicine choninic acid (BCA) as coloring reagent (*42*).

Calculation of Apparent Molecular Masses. For PSIIcc*Te*, PSIIcc*So*, and PSI*Te* molecular masses M_{cal} were calculated from the sum of the molecular masses of the polypeptides forming PSIIcc or PSI, including the molecular mass of the cofactors. The subunit compositions of fraction I and II of PSIIcc*Te* and upper and lower band of PSIIcc*So* have been determined by SDS/PAGE and MALDI-TOF-MS (see ref *10* and Figure S1, Supporting Information). The pigment composition for PSIIcc*Te* has been determined in ref *6*. The subunit composition and cofactor composition of PSIcc*Te* was determined previously by Jordan et al. (*41*). For trimeric LHCII a pigment content of 24 Chl*a*, 18 Chl*b*, and 12 Car was taken from the X-ray structure (*43*). The pigment contents were determined to be 6 Chl*a*, 2 Chl*b*, and 2−3 carotenes for CP29 and 14−15 Chl*a* and 3−4 carotenes for CP47. The molecular mass M_{Det} of *β*-DM and lipid molecules, forming the detergent belts around fraction I and II

Table 1: Molecular Weight of PSII Determined by GPC, AUC, and DLS[a]

protein	M_{cal}	M_{Det}	M_{cor}	M_{GPCA} (GPC fit A)	M_{GPCB} (GPC fit B)	M_{AUC} (anal. UC)	M_{DLS} (DLS)
CP29 spinach°	36	50	86	45 ± 3	93 ± 6		
CP47 spinach°	70	50	120	72 ± 2	122 ± 4		
LHC II spinach°	196	50	246	165 ± 20	225 ± 30		
PSI*Te*° (monomer)	356	90 ± 22	446	390 ± 15	480 ± 30		
PSI*Te*° (trimer)	1068	250 ± 50	1318	1055 ± 60	1300 ± 40	1016 ± 70 (0.04 mg/mL)	
PSIIcc*Te* (fraction I) (monomer)	343	90 ± 22	433	320 ± 20 (0.1 mg/mL)	400 ± 20 (0.1 mg/mL)	441 ± 10 (0.1 mg/mL)	
				320 ± 20 and 610 ± 43 (1.5 mg/mL)	400 ± 20 and 740 ± 55 (1.5 mg/mL)	1215 ± 28 (0.8 mg/mL)	1430 ± 87 (2 mg/ml)
PSIIcc*Te* (fraction II) (dimer)	686	126 ± 25	812	610 ± 43 (0.1 mg/mL)	740 ± 55 (0.1 mg/mL)	756 ± 18 (0.2 mg/mL)	426 ± 10 (<0.5 mg/mL)
							768 ± 40 (1 mg/mL)
							3600 ± 10 (3.34 mg/mL)
PSIIcc*So* upper band (monomer)	350	90 ± 22	440	300 ± 25 (0.1 mg/mL)	380 ± 30 (0.1 mg/mL)		
PSIIcc*So* lower band (dimer)	630	126 ± 25	756	560 ± 30 (0.1 mg/mL)	670 ± 40 (0.1 mg/mL)	710 ± 15 (0.2 mg/mL)	aggregates (0.05 mg/mL)

[a] All values are given in kDa ± σ. The protein concentrations used for mass determination by AUC and DLS are given in parantheses. M_{cal}: molecular mass calculated from sequence including cofactors. M_{Det}: mass of detergent belt estimated as described in Materials and Methods. M_{cor}: molecular mass including detergent ($M_{cal} + M_{Det}$). M_{GPCA}: molecular mass determined from gel permeation chromatography using M_{cal} as M of the calibration proteins for generating the fit curve A. M_{GPCB}: molecular mass determined from gel permeation chromatography using M_{cor} as M of the calibration proteins for generating the fit curve B. M_{AUC}: molecular mass determined from analytical ultracentrifugation. M_{DLS}: molecular mass determined from dynamic light scattering. The proteins marked with a degree symbol (°) were used for generating the fit curves for GPC.

of PSIIcc*Te*, was calculated from the values given in ref *6* to be 90 ± 22 kDa (fraction I) and 126 ± 25 kDa (fraction II). For trimeric PSI*Te*, M_{Det} was determined following the procedure described in ref *6* to be 250 ± 50 kDa (see Table 1). The M_{Det} for upper (monomer) and lower band (dimer) PSIIcc*So* were taken to be similar to the M_{Det} determined for PSIIcc*Te*. For monomeric PSI*Te*, the M_{Det} of monomeric PSIIcc*Te* was adopted due to the comparable size of both complexes. For the other antenna pigment−protein complexes (CP29, CP47, trimeric LHCII), M_{Det} was assumed to be similar to the pure β-DM micelle (98 β-DM molecules, 50 kDa (*44*)). The corrected total molar mass M_{cor} was obtained from the sum of M_{cal} and M_{Det} as given in Table 1.

Determination of the Partial Specific Volume, $\bar{\nu}$. Stock solutions of PSIIcc*Te* or PSIIcc*So* and PSI*Te* were diluted stepwise with buffer A, B, or C, respectively, and measured using a DMA 40 digital densitometer (Anton Paar K. G., Austria). The difference of the square of the period T of the resonance frequency between two solutions measured in the U-shaped resonator of DMA 40 is related to the difference in their density by

$$\Delta\rho = \rho_1 - \rho_2 = A(T_1^2 - T_2^2) \quad (1)$$

where $\Delta\rho$ is the difference in density between the solution to be measured and water, T_1 is the period of the resonance of the solution under study, T_2 is the corresponding value for water, and A is an apparatus constant.

The partial specific volume, $\bar{\nu}$, was calculated according to eq 2 (*45*),

$$\bar{\nu} = \frac{1}{\rho_0}\left(1 - \frac{\rho - \rho_0}{c}\right) \quad (2)$$

where ρ is the density of the solution at a protein concentration c, and ρ_0 is the density of the buffer in the absence of dissolved protein.

Gel Permeation Chromatography (GPC). An Äkta FPLC chromatography system (Amersham Biotech) equipped with a Superose 6 HR10/30 gel permeation column (Amersham Biotech) was used for molecular mass determinations. The column was equilibrated with buffer A for all samples, flow rate was 0.5 mL/min, and the UV absorption was monitored at 280 nm. The void volume was determined using blue dextran. The column was calibrated with membrane proteins CP29 (36 kDa), CP47 (70 kDa), and trimeric LHCII (196 kDa) from *S. oleracea* and trimeric (1068 kDa) and monomeric PSI*Te* (356 kDa). The value K_{av} was calculated according to eq 3,

$$K_{av} = \frac{V_e - V_0}{V_t - V_0} \quad (3)$$

with V_e = elution volume, V_0 = void volume, and V_t = total bed volume.

An exponential fit of K_{av} versus the molecular mass M yielded the calibration curve for molecular mass determinations. To generate the calibration curves, either M_{cal} calculated from the sequence (Figure 1, fit A) or a corrected M_{cor} including the mass of the detergent belt (Figure 1, fit B) was used for M. The respective values for M_{cal} and M_{cor} are given in Table 1. For each calibration protein K_{av} was averaged from at least 3 runs. For the mass determination of PSIIcc, K_{av} was the average of at least 6 different preparations. The protein concentration was about 0.1 mg/mL (estimated from the peak area at fwhm) for all samples (for fraction I of PSIIcc*Te* one additional GPC run at 1.5 mg/mL protein concentration was conducted).

Dynamic Light Scattering (DLS). For corrections of the raw data obtained with dynamic light scattering (DLS), the

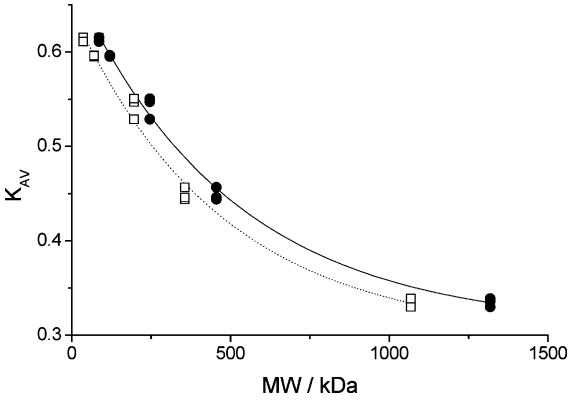

FIGURE 1: Calibration curves of gel permeation chromatography (GPC) using a set of membrane proteins as standards (see text): □ = membrane proteins (fit A), ● = membrane proteins + detergent belt (fit B).

refractive indices and viscosities of the solutions under study had to be determined. Refractive indices relative to air of all buffers and samples investigated were measured with an Atago refractometer at 20 ± 0.2 °C using light of the sodium D line. Differences in refractive indices at 525 nm were determined using a Brice−Phoenix differential refractometer (model BP-2000-V, Phoenix Precision Instrument Co., Philadelphia, PA) with a corresponding interference filter. The instrument was calibrated following the recommendations of the manufacturer. The protein concentration was varied between 0.1 and 2.0 mg/mL. Kinematic viscosities were determined using a capillary viscosimeter (type Ubbelohde, Schott, FRG) at 20 ± 0.5 °C, and the densities of the solutions were obtained with a digital densitometer DMA 40 (Anton Paar K.G., Austria) at 20 ± 0.2 °C.

Dynamic light scattering (DLS) or quasi elastic light scattering (QELS) was used to obtain directly the diffusion coefficient (D_z) of protein particles. The translational diffusion coefficient is obtained from the autocorrelation function of the scattered light. It permits the calculation of the hydrodynamic radius (R_H) of the protein particles by application of the Stokes−Einstein equation (eq 4),

$$R_H = \frac{k_B T}{6\pi\eta D_z} \tag{4}$$

where η, k_B, and T are the solvent viscosity, the Boltzmann constant, and the absolute temperature, respectively. The equation holds as long as the hydrodynamic radius, R_H, is small compared to the employed wavelength ($R_H < \lambda/20$).

Under the assumption that the protein particles are spherical and do not interact at zero concentration, the hydrodynamic particle radius (R_H) and the protein volume (V) are related by

$$V = (4/3)\pi {R_H}^3 \tag{5}$$

The molecular weight M is then simply related to the protein volume (V) by

$$M = (V/\bar{\nu})\times N_A \tag{6}$$

where $\bar{\nu}$ is the partial specific volume of the protein [cm^3/g] and N_A is Avogadro's number.

For DLS measurements, PSIIcc*Te* was dissolved in buffer A and passed through Millex sterile filters (0.22 μm pore size) into standard cylindrical light scattering cells. The protein concentration of PSIIcc*Te* was varied from 0.2 mg/mL to 3.34 mg/mL in buffer A, and the protein concentration of PSIIcc*So* (lower band) was varied from 0.2 mg/mL to 2 mg/mL in buffer B. The experiments were carried out at constant temperature (20 ± 0.2 °C), controlled by a Lauda RC6 thermostat and at a constant scattering angle of 20°. The volumes employed in these experiments were about 1 mL. DLS experiments were conducted with an ALV/SP-80 light scattering spectrogoniometer (ALV, Langen, Germany) and the ALV-5000/fast digital correlator with 286 channels spaced quasi-logarithmically in time. A frequence-doubled Nd:YAG laser operating at a wavelength of 532 nm served as the light source.

The particle distribution function for measured PSIIcc samples was obtained after Laplace inversion of the autocorrelation function with a modification of the program CONTIN (*46*, *47*). CONTIN provides a *z*-averaged relaxation rate distribution allowing for the calculation of the mean relaxation rate gamma (γ). Gamma is related to D_z by $\gamma/q^2 = D_z$.

Analytical Ultracentrifugation. The sedimentation equilibrium technique allows the determination of M according to

$$c_{(r)} = c_0\, e^{MF} \tag{7}$$

with

$$F = \frac{(1 - \rho\bar{\nu})\omega^2(r^2 - {r_0}^2)}{2RT} \tag{8}$$

where ρ is the solvent density, $\bar{\nu}$ the partial specific volume of the protein, ω the angular velocity, R the gas constant, T the absolute temperature, $c_{(r)}$ the radial concentration, and c_0 the corresponding value at the meniscus position. In addition to the molar mass, these parameters allow calculation of R_H, using eq 4, and of the volume, V, using eq 5. In aqueous solution, the radius is larger by about 0.3 nm (water shell).

Ultracentrifugation experiments were performed using an XL-A analytical ultracentrifuge (Beckman, Palo Alto, CA) equipped with absorbance optics. For determination of the molar mass M, the sedimentation equilibrium data were analyzed by means of externally loaded six-channel centerpieces of 12 mm optical path length filled with 70 μL of solution in the corresponding compartment. This cell type allows the analysis of three solvent/solution pairs. The concentrations of PSIIcc*Te* (fraction I and II), PSIIcc*So* (lower band), and PSI*Te* were adjusted to 10 μM Chl*a* throughout in buffer A, B, and C, respectively. The sedimentation equilibrium was reached after 2 h overspeed at 14000 rpm, followed by an equilibrium speed of 10000 rpm at 10 °C for about 30 h. The radial absorbances of each compartment were recorded at three different wavelengths between 400 and 700 nm for each protein under study. The molar mass determinations were done by simultaneously fitting the three radial distribution curves according to eqs 7 and 8 with the program POLYMOLE (*48*) applying the experimentally determined partial specific volume (see above).

RESULTS

Determination of Partial Specific Volume. The densities of PSIIcc*Te*, PSIIcc*So*, and PSI*Te* dissolved at various concentations in buffers A, B, and C, respectively, were measured. From the density measurements the partial specific volume, $\bar{\nu}$, was determined to be 0.76 cm^3/g for PSIIcc*Te* and PSI*Te*. For PSIIcc*So* in buffer B, no density measurement was possible due to the high sucrose concentration of the buffer. As the overall composition of PSIIcc*So* is very similar to PSIIcc*Te*, the value $\bar{\nu} = 0.76$ cm^3/g was also used for PSIIcc*So*.

Gel Permeation Chromatography. GPC analyses were carried out to determine the molecular masses of fractions I and II of PSIIcc*Te* and the two forms of PSIIcc*So*. The resulting molecular masses using the two different calibration curves (Figure 1) are shown in Table 1. For the pigment−protein complexes used for calibration, fits A and B (Figure 1) yielded molar masses that were in good agreement with the expected masses, either with or without the detergent belt, indicating that the obtained values could be fitted well by an exponential function. For fractions I and II of PSIIcc*Te*, fit B yielded masses M_{GPCB} of 400 ± 20 and 740 ± 55 kDa, respectively. For the two forms of PSIIcc*So*, 380 ± 30 and 670 ± 40 kDa were obtained. These values are within error in good agreement with the calculated M_{cor} (about 10% deviation) for monomeric and dimeric PSIIcc, respectively. When using fit A, based on M_{cal} of the calibration proteins without the detergent belt, the obtained values for M_{GPCA} were 80 to 130 kDa smaller (Table 1) compared to M_{GPCB}, but the deviation from M_{cal} was in the same order (approximately 10%). To study the aggregation behavior of fraction I of PSIIcc*Te*, a GPC experiment was conducted at 15 times higher protein concentration (1.5 mg/mL). Under these conditions a shoulder appeared with an elution volume V_e similar to V_e of fraction II of PSIIcc*Te*, indicating the formation of dimeric complexes. This shoulder accounted for about 4% of the total peak area, indicating that the vast majority of the protein was still in its monomeric state.

Dynamic Light Scattering (DLS). Throughout the light scattering experiments, the raw data obtained from the green PSIIcc solutions had to be corrected for light absorption and refractive index. These corrections were necessary because we used laser light at 532 nm where the PSIIcc solutions still exhibit some absorption. The corrections are based on two graphs where the optical density (Figure 2) and refractive index (Figure 3) are plotted as a function of PSIIcc dissolved in buffer A or B, respectively, in the protein concentration range between 0.1 and 2.0 mg/mL. Both graphs show linear dependence, suggesting that the PSIIcc solutions behave "normally" in the chosen concentration range.

The hydrodynamic radius R_H of PSIIcc (eq 4) was derived from the diffusion coefficient D_z determined by DLS. DLS experiments using fraction I of PSIIcc*Te* at high concentrations of 2 mg/mL yielded a diffusion coefficient of 2.70 ± 0.03 × 10^{-7} cm^2 s^{-1}. This value corresponds to a hydrodynamic radius, R_H, of 7.85 ± 0.15 nm and an apparent molecular mass M_{DLS} of 1430 ± 87 kDa according to eqs 4 to 6. For fraction II of PSIIcc*Te*, a diffusion coefficient of 3.0 ± 0.03 × 10^{-7} cm^2 s^{-1} was determined at a protein concentration of 1 mg/mL (Figure 4). This value corresponds to $R_H = 6.14 \pm 0.15$ nm and a molar mass M_{DLS} of 768 ± 40 kDa. In addition, the concentration dependence of D_z in the range between 0.015 and 3.34 mg/mL was measured for fraction II of PSIIcc*Te* (Figure 5). At low protein concentrations (between 0.015 and 0.5 mg/mL) the diffusion coefficient D_z was roughly constant at 3.7 ± 0.2 × 10^{-7} cm^2 s^{-1}. For protein concentrations between 0.5 mg/mL and 3.34 mg/mL the diffusion coefficient decreased linearly to 1.65 ± 0.2 × 10^{-7} cm^2 s^{-1}. The diffusion coefficients corresponded to R_H values between 5.02 ± 0.15 nm and 13 ± 0.2 nm or to apparent molecular masses M_{DLS} between 4.26

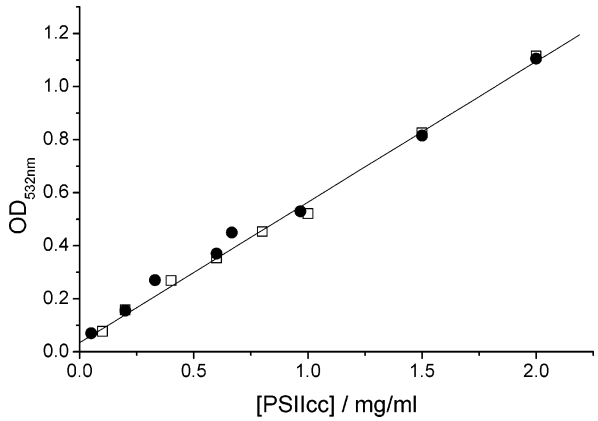

FIGURE 2: Dependence of the absorption (OD) at 532 nm on the protein concentration of fraction II PSIIcc*Te* (●) and lower band PSIIcc*So* (□) dissolved in buffer A and B, respectively.

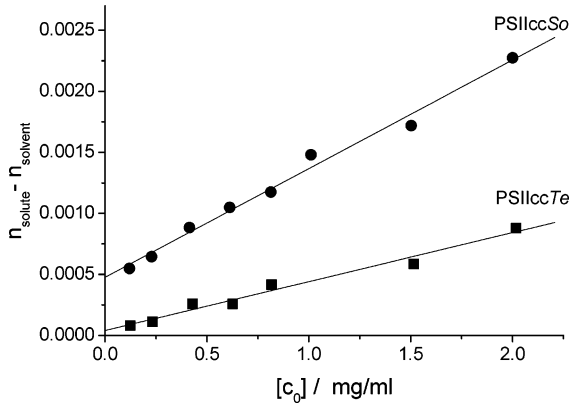

FIGURE 3: Refractive index *n* as a function of PSIIcc*Te* (lower curve) and PSIIcc*So* (upper curve) protein concentrations in buffer A and B, respectively.

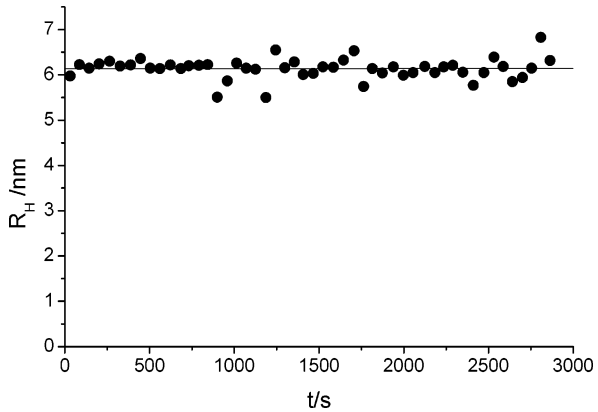

FIGURE 4: Hydrodynamic radius R_H determined by DLS as a function of time. The protein concentration of PSIIcc*Te* (fraction II) was 1 mg/mL in buffer A. Spectra were collected at a scattering angle of 20°. $R_H = 6.14 \pm 0.15$ nm.

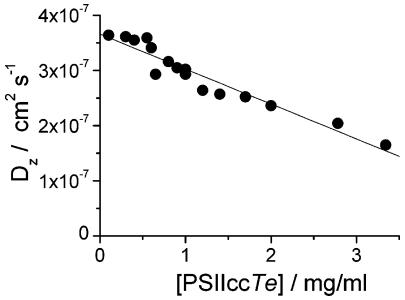

FIGURE 5: Dependence of the diffusion coefficient D_z on the protein concentration of PSIIcc*Te* (fraction II) dissolved in buffer A.

$\pm$ 0.1 $\times$ 10^5 g/mol and 36 $\pm$ 0.1 $\times$ 10^5 g/mol. This increase of the R_H values with higher protein concentrations suggests attractive interactions between PSII particles leading to the formation of small aggregates with molecular weights of 36 $\times$ 10^5 g/mol (corresponding to nonamers) or less. These aggregates represent the major population at higher concentrations of PSIIcc*Te*. No smaller PSIIcc particles could be observed once a protein concentration of 3.34 mg/mL had been reached.

A R_H of about 30 $\pm$ 0.35 nm was determined for the lower band of PSIIcc*So* at a protein concentration of 0.5 mg/mL. This indicated that even at low concentrations of lower band PSIIcc*So* ill-defined very large aggregates were formed (data not shown). This is supported by the observed nonlinear dependence between lower band PSIIcc*So* at protein concentrations between 0.2 and 2 mg/mL and R_H values.

Analytical Ultracentrifugation. On the basis of the radial distributions from analytical ultracentrifugation experiments the molar masses, M_{AUC}, of fractions I and II from PSIIcc*Te* and of lower band from PSIIcc*So* were determined.

For fraction I of PSIIcc*Te* M_{AUC} = 1215 $\pm$ 28 kDa was determined in the protein concentration range 0.65−0.875 mg/mL. Additional analytical ultracentrifugation experiments in the protein concentration range between 0.03 and 0.11 mg/mL of fraction I of PSIIcc*Te* yielded a M_{AUC} of 441$\pm$ 10 kDa.

Fraction II of PSIIcc*Te* and the lower band of PSIIcc*So* exist in dilute solution at protein concentrations below 0.2 mg/mL as dimers with molar masses, M_{AUC}, of 756 $\pm$ 18 kDa and 710 $\pm$ 15 kDa, respectively (Figure 6a,b). Only at very low protein concentrations below 0.05 mg/mL did fraction II of PSIIcc*Te* partially dissociate (20−30%) into monomers. The resulting monomers are unstable under these conditions and start to aggregate forming heterogeneous particles.

As a control, the molar mass of PSI*Te* was measured by analytical ultracentrifugation in the same concentration range as applied for PSIIcc, yielding a value M_{AUC} of 1016 $\pm$ 70 kDa for the PSI*Te* trimer.

For fraction I of PSIIcc*Te* the determined M_{UCA} at low protein concentrations agrees well with the M_{cor} for monomeric PSIIcc (Table 1). The values of M_{UCA} determined for fraction II of PSIIcc*Te* and the lower band of PSIIcc*So* at a protein concentration of 0.2 mg/mL are in good agreement with the respective M_{cor} for dimeric PSIIcc. The M_{UAC} for trimeric PSI*Te* is smaller than the expected M_{cor} (Table 1). This difference could be due to either an overestimation of the detergent belt in calculating M_{cor} for PSI or an error in the determination of the partial molar volume for PSI*Te*.

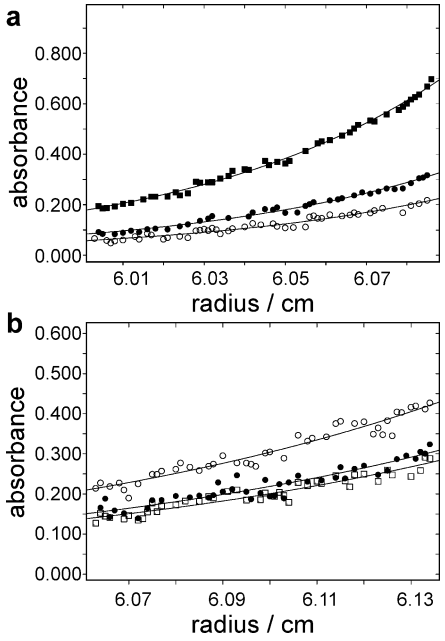

FIGURE 6: Radial distribution functions of the sedimentation equilibrium technique for PSIIcc from (a) *T. elongatus* (fraction II) and (b) *S. oleracea* (lower band) at a protein concentration of 0.2 mg/mL each. Detection wavelengths: (a) ■ = 675 nm, ● = 500 nm, ○ = 642 nm; (b) □ = 699 nm, ● = 696 nm, ○ = 693 nm.

DISCUSSION

Three approaches have been used in the present study to estimate the molecular masses of the oxygen evolving PSIIcc*Te* and PSIIcc*So*: GPC, DLS and analytical ultracentrifugation.

The molecular mass of PSIIcc as determined by GPC corresponds to the protein covered by detergent. The molecular masses of fraction I and fraction II from PSIIcc*Te* with detergent were estimated to be M_{GPCB} = 400 $\pm$ 20 kDa and 740 $\pm$ 55 kDa (Table 1), respectively, using fit B. These values indicate that fraction I of PSIIcc*Te* corresponds to the monomeric and fraction II to the dimeric form. For PSIIcc*So*, M_{GPCB} values of 380 $\pm$ 30 kDa and 670 $\pm$ 40 kDa (Table 1) for the upper band and lower band were determined, respectively. In analogy to fraction I and II of PSIIcc*Te*, the M_{GPCB} values of PSII*So* indicate that the upper band corresponds to the monomeric and the lower band to the dimeric form. The difference of about 20−35 kDa in molecular mass per monomer between PSIIcc*Te* and PSIIcc*So* is mainly due to the loss of the two smaller extrinsic proteins (PsbP and PsbQ) during the purification of PSIIcc*So*, whereas PSIIcc*Te* retains the extrinsic subunits PsbU and PsbV with molecular masses of 12 and 15 kDa, respectively (see ref *10* and Figure S1).

Several groups reported sizes of monomeric and dimeric PSIIcc determined by GPC. Rögner et al. and Kuhl et al. reported 300 kDa for monomeric and 500 kDa for dimeric PSIIcc*Te* (*13*, *25*). Shen and Kamiya (*26*) reported for monomeric PSIIcc from rice a size of 380 kDa and a size of 580 kDa for the dimeric PSIIcc from *T. vulcanus*. Sugiura and Inoue reported masses of 350 and 580 kDa, respectively, for the monomeric and dimeric His-tagged PSIIcc*Te* (*49*). Calibrating the GPC with soluble proteins and neglecting the detergent belt in size determination can explain the

differences between the data reported in this study and the data for the size of monomeric and dimeric PSIIcc obtained by GPC by various other groups. Especially the size of the dimeric PSIIcc is underestimated in all of these studies and comparable to the value we obtained when neglecting the detergent belt for mass calibration (M_{GPCA} = 610 kDa).

Compared with literature data and the expected masses from the primary structure of the subunits and cofactors, the calibration of GPC columns using membrane proteins instead of soluble proteins and considering the detergent belt yields more realistic values for the size of the monomeric and dimeric PSIIcc from *S. oleracea* and *T. elongatus*.

Dynamic Light Scattering. The best way to obtain information about the aggregation state of a protein in solution is to determine its hydrodynamic radius, R_H, as a function of protein concentration by DLS. This also provides a good indication for potential crystallization of a protein solution (*50*), because random aggregation may prevent formation of ordered nuclei that are necessary for crystal growth.

DLS on diluted solutions of PSIIcc*Te* has been used to determine the diffusion coefficients and molecular masses. A very interesting point of the DLS measurements concerns the aggregation behavior of the PSIIcc*Te* particles in solution, which is well documented by the concentration dependence of the diffusion coefficient of PSIIcc*Te* (fraction II) shown in Figure 5. The diffusion coefficient D_z decreases linearly from $3.7 \pm 0.2 \times 10^{-7}$ cm^2 s^{-1} to $1.65 \pm 0.2 \times 10^{-7}$ cm^2 s^{-1}, corresponding to R_H values between 5.02 ± 0.15 and 13 ± 0.2 nm. Extrapolating to a PSIIcc protein concentration of zero, an apparent molecular mass of 400 ± 20 kDa is obtained. By contrast, at a higher PSIIcc*Te* (fraction II) protein concentration of 3.34 mg/mL the R_H value increases to 13 ± 0.2 nm, indicating an apparent molecular mass of 3600 kDa. This observation suggests that at low PSIIcc*Te* protein concentrations PSIIcc*Te* monomers predominate, but at higher PSIIcc*Te* protein concentrations small aggregates from monomer to nonamer are formed. At medium protein concentrations of 1 mg/mL, a D_z corresponding to a mass of 786 kDa was found, indicating the presence of dimeric complexes. Many authors have studied the dependence of the diffusion coefficient of a protein on its concentration (*51*) and pointed out that interparticle interactions play an important role in the formation of protein aggregates. Four parameters define the interactions between hard spheres in solution: the size of the spheres, the repulsive interactions defined by the net charge of the particles, the interaction strength defined by the Debye length, and the attractive potential (*51*−*53*). The surface potential is a key factor determining the interaction between two protein particles. In our case the surface potential of PSIIcc*Te* is unknown and cannot be calculated because a model of PSIIcc*Te* at a reliable atomic resolution is not yet available.

The aggregation behavior of lower band PSIIcc*So* has also been studied using DLS. The dependence of the hydrodynamic radius R_H on the PSIIcc*So* concentration is sigmoidal, indicating a rapid (and cooperative) increase from PSIIcc*So* monomers at a low PSIIcc*So* protein concentration (0.2 mg/mL) to ill-defined and very large aggregates at higher PSIIcc*So* protein concentrations (data not shown). This extreme aggregation behavior of PSIIcc*So* may be associated with the predominantly hydrophobic character as this PSIIcc contains only one hydrophilic subunit, PsbO. By contrast no formation of large aggregates is observed for PSIIcc*Te* (fraction II) at low to medium concentrations due to 3 hydrophilic charged subunits (PsbO, Cyt c550, PsbU) located externally to the membrane, which lead to electrostatic repulsion. At higher PSIIcc*Te* concentrations, however, smaller aggregates (from dimer to nonamer) begin to form (Figure 5).

A Critical Point of View Concerning the Results from the DLS Experiments. The calculation of the hydrodynamic radius, R_H, from the measured diffusion coefficients, D_z, depends in general on the assumption of a spherical form of the macromolecule. DLS experiments are unable to distinguish between monomers and dimers, since the increase in the hydrodynamic radius upon dimerization is only 20%, which is of the same order of magnitude as the experimental error typical for DLS experiments. The calculation of the hydrodynamic radii of PSIIcc*Te* according to eqs 5 and 6 applying molar masses of 433 and 805 kDa resulted in R_H values of 5.07 and 6.23 nm for monomeric and dimeric PSIIcc*Te*, respectively. The calculated value of 5.07 nm for monomeric PSIIcc*Te* is close to R_H of 5.02 ± 0.15 found for low concentrations of fraction II PSIIcc*Te*.

As the normal assumption of a spherical molecule is not valid for the membrane protein complexes studied here, we tried to calculate the diffusion coefficient for monomeric PSIIcc from the atomic coordinates available. Using an Oseen tensor (*54*) the diffusion coefficient was calculated from the coordinates of the Cα atoms of monomeric PSIIcc*Te* (pdb: 1FE1) to be D_z trans = 4.36×10^{-7} cm^2 s^{-1} at RT. Using a Rotne−Prager tensor $D_z = 4.77 \times 10^{-7}$ cm^2 s^{-1} was obtained (*55*). These values are larger than the observed D_z for fraction II of PSIIcc*Te* at low concentrations, indicating that the molecular weight of 426 kDa calculated from the observed D_z value has to be taken with care.

Analytical Ultracentrifugation (AUC). The molar mass determined by sedimentation equilibrium does not depend on the form of the molecule, whereas in DLS experiments usually a spherical form of the macromolecules under study is assumed.

The results for fraction I of PSIIcc*Te* at low concentrations support the assignment of this fraction to monomeric PSIIcc derived from the GPC data (M_{AUC} and M_{GPCB} are within error similar). At higher concentrations the masses found are in accordance with the results from DLS, indicating the formation of large aggregates from fraction I of PSIIcc*Te*. In contrast this aggregation is not visible when using GPC (see Table 1), demonstrating that GPC is not the method of choice to investigate aggregation behavior of the membrane proteins studied.

In contrast to the results from the DLS measurements on fraction II of PSIIcc*Te*, the results of analytical ultracentrifugation experiments have clearly demonstrated the occurrence of PSIIcc*Te* dimers even at low protein concentrations <0.2 mg/mL and must be considered as superior to DLS if accurate molar masses have to be determined. At very low protein concentrations of 0.05 mg/mL the PSIIcc*Te* dimers are unstable and tend to dissociate into monomers while at higher protein concentrations (0.8 mg/mL) aggregation of dimeric PSIIcc*Te* takes place. For the lower band of PSIIcc*So* again the value of M_{AUC} obtained via analytical ultracentrifugation is close to the expected M_{cor} for the dimeric complex and similar to M_{GPCB} (Table 1).

To obtain a reliable value for M_{AUC} the partial molar volume, $\bar{\nu}$, is crucial. It has to be either experimentally determined, as in our case, or calculated from the exact composition of the studied complex. The range of $\bar{\nu}$ values for soluble proteins is 0.70 to 0.75 $cm^3\ g^{-1}$, and normally the mean of 0.73 $cm^3\ g^{-1}$ is used (*56*). For PSII and PSI the determined value of 0.76 $cm^3\ g^{-1}$ is above the reported range for soluble proteins but in excellent agreement with $\bar{\nu} = 0.757\ cm^3\ g^{-1}$, as estimated by Lustig et al. for several membrane proteins such as PSIIcc, reaction center of *R. sphaeroides* R26 and OmpF-porin, thus demonstrating the necessity of using the appropriate value of $\bar{\nu}$ (*57*).

CONCLUSIONS

In the present work, using gel permeation chromatography and analytical ultracentrifugation, fractions I and II from PSIIcc of *T. elongatus* and the upper and lower bands of *S. oleracea* have been identified as monomeric and dimeric PSIIcc, respectively.

The essence of the described experiments is that they show PSIIcc*Te* to occur predominantly as relatively small aggregates in solution, similar to those generally observed for well-crystallizing proteins (*58*). This was taken as an indication that crystallization might be achieved under comparable experimental conditions, although the light scattering studies were restricted to PSIIcc*Te* protein concentrations below or at 3.34 mg/mL. At higher protein concentrations, the optical absorption increased nonlinearly due to inner filter effects and became so strong that light scattering experiments had to be abolished. Since crystallization with polyethylene glycol as the precipitating agent requires PSIIcc*Te* protein concentrations of at least 10 mg/mL (*6*, *59*), i.e., significantly higher than the 3.34 mg/mL employed in the present DLS study, it can be assumed that the formation of larger aggregates would be even more favored and that dimeric PSIIcc*Te* would be consumed by growing nuclei.

The three-dimensional crystals obtained are capable of water oxidation, indicating that PSIIcc*Te* is in a fully native, enzymatically active state (*60*). The crystals diffract synchrotron X-rays to a resolution of 3.2 Å and contain PSII homodimers (*39*). This agrees with the analytical ultracentrifugation experiments, which suggest that fraction II of PSIIcc*Te* occurs as a dimer in solution under the conditions employed in these studies. We emphasize that under different conditions in solution or embedded in the thylakoid membrane, PSIIcc*Te* could adopt other aggregation forms.

In contrast to PSIIcc*Te* dimer, monomeric PSIIcc*Te* aggregates even at low protein concentrations, and no 3D crystals have been reported so far. The behavior of PSIIcc*Te* differs largely from that observed for lower band dimeric PSIIcc*So* where large, ill-defined aggregates are observed by DLS even at low protein concentrations (0.05 mg/mL). The formation of large aggregates is probably associated with the structure of PSIIcc*So* which features only one membrane-extrinsic subunit PsbO whereas the other two hydrophilic membrane-extrinsic subunits found in PSIIcc*Te*, PsbU and PsbV, are missing.

Despite these unfavorable properties of PSIIcc*So* for crystallization experiments, crystals of dimeric PSII-RC*So* and monomeric PSIIcc*So* were obtained. However, crystals of dimeric PSII-RC*So* did not diffract X-rays beyond 15 Å resolution (*61*). The crystals of PSIIcc*So* were of better quality, but the resolution limit of 6.5 Å was still too low to proceed with the X-ray analysis (*62*, *63*). The low resolution X-ray diffraction of PSII-RC*So* and PSIIcc*So* is probably associated with heterogeneity in posttranslational modification that may lead to heterogeneous aggregation (*27*, *64*−*67*). Such problems did not arise with PSIIcc*Te*, and we assume that this is the reason the obtained crystals are qualitatively superior to those grown from monomeric PSIIcc*So* and dimeric PSII-RC*So*.

In summary, we have shown in this study that the determination of the aggregation behavior of detergent-solubilized membrane-intrinsic proteins is a prerequisite for successful crystallization experiments. Besides GPC calibrated with membrane proteins, a combination of DLS and analytical ultracentrifugation is recommended to determine unambiguously the size and concentration dependent change of the oligomerization state of a membrane protein in solution.

ACKNOWLEDGMENT

The authors are grateful to Dr. Y. Georgalis for valuable discussions and for initiating the DLS experiments, and they thank D. DiFiore, C. Lüneberg, K. Scharf, and S. Kussin for technical assistance and Dr. R. Clarke for careful reading of the manuscript.

SUPPORTING INFORMATION AVAILABLE

Figure S1, the SDS−PAGE of *T. elongatus* and spinach monomeric and dimeric PSIIcc, showing the subunit composition of all four complexes investigated. This material is available free of charge via the Internet at http://pubs.acs.org.

REFERENCES

1. Peterman, E. J. G., van Amerongen, H., van Grondelle, R., and Dekker, J. P. (1998) The nature of the excited state of the reaction center of photosystem II of green plants: A high-resolution fluorescence spectroscopy study, *Proc. Natl. Acad. Sci. U.S.A. 95*, 6128−6133.
2. Barter, L. M., Durrant, J. R., and Klug, D. R. (2003) A quantitative structure-function relationship for the photosystem II reaction center: Supermolecular behavior in natural photosynthesis, *Proc. Natl. Acad. Sci. U.S.A. 100*, 946−951.
3. Renger, G. (2001) Photosynthetic water oxidation to molecular oxygen: apparatus and mechanism, *Biochim. Biophys. Acta 1503*, 210−228.
4. Barber, J. (2003) Photosystem II: the engine of life, *Q. Rev. Biophys. 36*, 71−89.
5. Ke, B. (2001) *Photosynthesis—Photobiochemistry and Photobiophysics*, Vol. 10, Kluwer Academic, Dordrecht.
6. Kern, J., Loll, B., Lüneberg, C., DiFiore, D., Biesiadka, J., Irrgang, K.-D., and Zouni, A. (2005) Preparation, characterisation and crystallisation of photosystem II from Thermosynechococcus elongatus, *Biochim. Biophys. Acta, 1706*, 147−157.
7. Nanba, O., and Satoh, K. (1987) Isolation of a photosystem II reaction center consisting of D-1 and D-2 polypeptides and cytochrome b-559, *Proc. Natl. Acad. Sci. U.S.A. 84*, 109−112.
8. Gounaris, K., Chapman, D. J., and Barber, J. (1989) Isolation and characterisation of D1/D2/cytochrome b559 complex from Synechocystis 6803, *Biochim. Biophys. Acta 973*, 296−301.
9. Seidler, A. (1996) The extrinsic polypeptides of Photosystem II, *Biochim. Biophys. Acta 1277*, 35−60.
10. Kern, J., Zouni, A., Franke, P., Schröder, W., and Irrgang, K.-D. (2004) Subunit composition of Photosystem II Core Complexes from the cyanobacterium *Thermosynechococcus elongatus* and the higher plant *Spinacia oleracea*, *Plant J.*, submittted.

11. Shi, L. X., and Schröder, W. P. (2004) The low molecular mass subunits of the photosynthetic supracomplex, photosystem II, *Biochim. Biophys. Acta 1608*, 75−96.
12. Haag, E., Irrgang, K.-D., Boekema, E. J., and Renger, G. (1990) Functional and structural analysis of photosystem II core complexes from spinach with high oxygen evolution capacity, *Eur. J. Biochem. 189*, 47−53.
13. Rögner, M., Dekker, J. P., Boekema, E. J., and Witt, H. T. (1987) Size, Shape and mass of the oxygen-evolving photosystem II complex from the thermophilic cyanobacterium *Synechococcus* sp., *FEBS Lett. 219*, 207−211.
14. Lustig, A., Engel, A., and Zulauf, M. (1991) Density determination by analytical ultracentrifugation in a rapid dynamical gradient: application to lipid and detergent aggregates containing proteins, *Biochim. Biophys. Acta 1115*, 89−95.
15. Holzenburg, A., Bewly, M. C., Wilson, F. H., Nicholson, W. V., and Ford, R. (1993) Three-dimensional structure of photosystem II, *Nature 363*, 470−472.
16. Ford, R. C., Rosenberg, M. F., Shepherd, F. H., McPhie, P., and Holzenburg, A. (1995) Photosystem II 3-D structure and the role of the extrinsic subunits in photosynthetic oxygen evolution, *Micron 26*, 133−140.
17. Tsiotis, G., Walz, T., Spyridaki, A., Lustig, A., Engel, A., and Ghanotakis, D. (1996) Tubular crystals of a photosystem II core complex, *J. Mol. Biol. 259*, 241−248.
18. Bassi, R., Ghiretti Magaldi, A., Tognon, G., Giacometti, G. M., and Miller, K. R. (1989) Two-dimensional crystals of the photosystem II reaction center complex from higher plants, *Eur. J. Cell. Biol. 50*, 84−93.
19. Lyon, M. K., Marr, K. M., and Furcinitti, P. S. (1993) Formation and characterization of two-dimensional crystals of photosystem II, *J. Struct. Biol. 110*, 133−140.
20. Santini, C., Tidu, V., Tognon, G., Ghiretti Magaldi, A., and Bassi, R. (1994) Three-dimensional structure of the higher-plant photosystem II reaction centre and evidence for its dimeric organization in vivo, *Eur. J. Biochem. 221*, 307−315.
21. Boekema, E. J., Hankamer, B., Bald, D., Kruip, J., Nield, J., Boonstra, A. F., Barber, J., and Rögner, M. (1995) Supramolecular structure of the photosystem II complex from green plants and cyanobacteria, *Proc. Natl. Acad. Sci. U.S.A. 92*, 175−179.
22. Marr, K. M., Mastronarde, D. N., and Lyon, M. K. (1996) Two-dimensional crystals of photosystem II: biochemical characterization, cryoelectron microscopy and localization of the D1 and cytochrome b559 polypeptides, *J. Cell Biol. 132*, 823−833.
23. Nield, J., Funk, C., and Barber, J. (2000) Supermolecular structure of photosystem II and location of the PsbS protein, *Philos. Trans. R. Soc. London, Ser. B: Biol. Sci. 355*, 1337−1344.
24. Yakushevska, A. E., Jensen, P. E., Keegstra, W., van Roon, H., Scheller, H. V., Boekema, E. J., and Dekker, J. P. (2001) Supermolecular organization of photosystem II and its associated light harvesting antenna in *Arabidopsis thaliana*, *Eur. J. Biochem. 268*, 6020−6028.
25. Kuhl, H., Kruip, J., Seidler, A., Krieger-Liszkay, A., Bunker, M., Bald, D., Scheidig, A. J., and Rögner, M. (2000) Towards structural determination of the water-splitting enzyme. Purification, crystallization, and preliminary crystallographic studies of photosystem II from a thermophilic cyanobacterium, *J. Biol. Chem. 275*, 20652−20659.
26. Shen, J. R., and Kamiya, N. (2000) Crystallization and the crystal properties of the oxygen-evolving photosystem II from *Synechococcus vulcanus*, *Biochemistry 39*, 14739−14744.
27. Tsiotis, G., McDermott, G., and Ghanotakis, D. (1996) Progress towards structural elucidation of Photosystem II, *Photosynth. Res. 50*, 93−101.
28. Ghanotakis, D. F., Tsiotis, G., and Bricker, T. M. (1999) Polypeptides of Photosystem II, in *Concepts in Photobiology: Photosynthesis and Photomorphogenesis* (Singhal, G. S., Renger, G., Sopory, S. K., Irrgang, K.-D., Govindjee, Eds.) pp 264−291, Narosa Publishing House, New Dehli, India.
29. Irrgang, K.-D., Lekauskas, A., Franke, P., Reifarth, F., Smolian, H., Karge, M., and Renger, G. (1998) in *Photosynthesis, Mechanisms and Effects* (Garab, G., Ed.) Vol. II, pp 977−980, Kluwer, Budapest.
30. Schatz, G. H., and Witt, H. T. (1984) Extraction and characterisation of oxygen-evolving Photosystem II complexes from a thermophilic cyanobacterium *Synechococcus* spec., *Photobiochem. Photobiophys. 7*, 1−14.
31. Fromme, P., and Witt, H. T. (1998) Improved isolation and crystallization of photosystem I for structural analysis, *Biochim. Biophys. Acta 1365*, 175−184.
32. Jekow, P., Fromme, P., Witt, H. T., and Saenger, W. (1995) Photosystem I from *Synechococcus elongatus*: preparation and crystallization of monomers with varying subunit compositions, *Biochim. Biophys. Acta 1229*, 115−120.
33. Henrysson, T., Schröder, W. P., Åkerlund, H.-E., and Spangfort, M. (1989) Isolation and characterization of the Chl a/b protein complex CP29 from spinach, *Biochim. Biophys. Acta 977*, 301−308.
34. Pieper, J., Irrgang, K. D., Rätsep, M., Voigt, J., Renger, G., and Small, G. J. (2000) Assignment of the lowest Q_Y-state and spectral dynamics of the CP29 chlorophyll a/b antenna complex of green plants: a hole-burning study, *Photochem. Photobiol. 71*, 574−581.
35. Huyer, J., Eckert, H.-J., Eichler, H. J., Irrgang, K.-D., Miao, J., and Renger, G. (2004) Fluorescence Decay Kinetics of Solubilized Pigment Protein Complexes from the Distal, Proximal, and Core Antenna of Photosystem II in the Range of 10−277 K and Absence or Presence of Sucrose, *J. Phys. Chem. B 108*, 3326−3334.
36. Irrgang, K.-D., Boekema, E. J., Vater, J., and Renger, G. (1988) Structural determination of the photosystem II core complex from spinach, *Eur. J. Biochem. 178*, 209−217.
37. Vasil'ev, S., Irrgang, K.-D., Schrötter, T., Bergmann, A., Eichler, H. J., and Renger, G. (1997) Quenching of chlorophyll a fluorescence in the aggregates of LHCII: steady-state fluorescence and picosecond relaxation kinetics, *Biochemistry 36*, 7503−7512.
38. Porra, R. J., Thompson, W. A., and Kriedemann, P. E. (1989) Determination of accurate extinction coefficients and simultaneous-equations for assaying chlorophyll *a* and chlorophyll *b* extracted with 4 different solvents—verification of the concentration of chlorophyll standards by atomic absorption spectroscopy, *Biochim. Biophys. Acta 975*, 384−394.
39. Biesiadka, J., Loll, B., Kern, J., Irrgang, K.-D., and Zouni, A. (2004) Crystal structure of cyanobacterial photosystem II at 3.2 Å resolution: a closer look at the Mn-cluster, *Phys. Chem. Chem. Phys. 6*, 4733−4736.
40. Barry, B. A., Boerner, R. J., and de Paula, L. C. (1994) The Use of Cyanobacteria in the Study of the Structure and Function of Photosystem II, in *The Molecular Biology of Cyanobacteria* (Bryant, D. A., Ed.) pp 217−257, Kluwer Academic Publishers, Dordrecht, Netherlands.
41. Jordan, P., Fromme, P., Witt, H. T., Klukas, O., Saenger, W., and Krauss, N. (2001) Three-dimensional structure of cyanobacterial photosystem I at 2.5 Å resolution, *Nature 411*, 909−917.
42. Brown, R. E., Jarvin, K. L., and Hyland, K. J. (1989) Protein measurement using bicinchoninic acid: elimination of interfering substances, *Anal. Biochem. 180*, 136−139.
43. Liu, Z., Yan, H., Wang, K., Kuang, T., Zhang, J., Gui, L., An, X., and Chang, W. (2004) Crystal structure of spinach major light-harvesting complex at 2.72 Å resolution, *Nature 428*, 287−292.
44. Rosevear, P., VanAken, T., Baxter, J., and Ferguson-Miller, S. (1980) Alkyl glycoside detergents: a simpler synthesis and their effects on kinetic and physical properties of cytochrome *c* oxidase, *Biochemistry 19*, 4108−4115.
45. Behlke, J. (1971) Über einige Erfahrungen mit der digitalen Dichtemesseinrichtung DMA 10 zur Bestimmung des partiellen spezifischen Volumens von Haemoglobin, *Stud. Biophys. 28*.
46. Provencher, S. W. (1982) A constrained regularization method for inverting data represented by linear algebraic of integral equations, *Comput. Phys. Commun. 27*, 213−228.
47. Provencher, S. W. (1982) CONTIN: A general purpose constrained regularization program for inverting noisy linear algebraic and integral equations, *Comput. Phys. Commun. 27*, 229−242.
48. Behlke, J., Ristau, O., and Schonfeld, H. J. (1997) Nucleotide-dependent complex formation between the Escherichia coli chaperonins GroEL and GroES studied under equilibrium conditions, *Biochemistry 36*, 5149−5156.
49. Sugiura, M., and Inoue, Y. (1999) Highly purified thermo-stable oxygen-evolving photosystem II core complex from the thermophilic cyanobacterium *Synechococcus elongatus* having His-tagged CP43, *Plant Cell Physiol. 40*, 1219−1231.
50. Georgalis, Y., Giri, L., and Littlechild, J. A. (1981) Physical studies on the ribosomal protein-S2 from the Escherichia coli 30S subunit, *Biochemistry 20*, 1061−1064.

51. Xia, J. Z., Aerts, T., Donceel, K., and Clauwaert, J. (1994) Light scattering by bovine alpha-crystallin proteins in solution: hydrodynamic structure and interparticle interaction, *Biophys. J. 66*, 861−872.
52. Verwey, E. J. W., and Overbeek, J. T. G. (1948) *Theory of the Stability of Lyophobic Colloids*, Amsterdam, 205 pp.
53. Wills, P. R., and Georgalis, Y. (1981) Concentration dependence of the diffusion coefficient of a dimerizing Protein: Bovine pancreatic trypsin inhibitor, *J. Phys. Chem. 85*, 3978−3983.
54. de la Torre, G. J., and Bloomfield, V. A. (1981) Hydrodynamic properties of complex, rigid, biological macromolecules—theory and applications, *Q. Rev. Biophys. 14*, 81−139.
55. Rotne, J., and Prager, S. (1969) Variational treatment of hydrodynamic interaction in polymers, *J. Chem. Phys. 50*, 4831−4837.
56. Harpaz, Y., Gerstein, M., and Chothia, C. (1994) Volume changes on protein folding, *Structure 2*, 641−649.
57. Lustig, A., Engel, A., Tsiotis, G., Landau, E. M., and Baschong, W. (2000) Molecular weight determination of membrane proteins by sedimentation equilibrium at the sucrose or Nycodenz-adjusted density of the hydrated detergent micelle, *Biochim. Biophys. Acta 1464*, 199−206.
58. Veesler, S., Marq, S., Lafont, S., Astier, J. P., and Boistelle, R. P. (1994) Influence of polydispersity on protein crystallization: a quasi-elastic light-scattering study applied to α-amylase, *Acta Crystallogr. D50*, 355−360.
59. Zouni, A., Lüneberg, C., Fromme, P., Schubert, W. D., Saenger, W., and Witt, H. T. (1998) Characterization of single crystals of Photosystem II from the thermophilic cyanobacterium *Synechococcus elongatus*, in *Photosynthesis: Mechanisms and Effects* (Garab, G., Ed.) Vol. II, pp 925−928, Kluwer Academic, Dordrecht.
60. Zouni, A., Jordan, R., Schlodder, E., Fromme, P., and Witt, H. T. (2000) First photosystem II crystals capable of water oxidation, *Biochim. Biophys. Acta 1457*, 103−105.
61. Fotinou, C., Kokkinidis, M., Fritzsch, G., Haase, W., Michel, H., and Ghanotakis, D. F. (1993) Characterization of a photosystem II core and its three-dimensional crystals, *Photosynth. Res. 37*, 41−48.
62. Adir, N., Okamura, M. Y., and Feher, G. (1992) Crystallization of the PSII-reaction centre, in *Research in Photosynthesis* (Murata, N., Ed.) pp 195−198, Kluwer Academic Press, Dordrecht, The Netherlands.
63. Adir, N. (1999) Crystallization of the oxygen-evolving reaction centre of photosystem II in nine different detergent mixtures, *Acta Crystallogr. D55*, 891−894.
64. Nugent, J. H. (1996) Oxygenic photosynthesis. Electron transfer in photosystem I and photosystem II, *Eur. J. Biochem. 237*, 519−531.
65. Sharma, J., Panico, M., Barber, J., and Morris, H. R. (1997) Characterization of the low molecular weight photosystem II reaction center subunits and their light-induced modifications by mass spectrometry, *J. Biol. Chem. 272*, 3935−3943.
66. Zheleva, D., Sharma, J., Panico, M., Morris, H. R., and Barber, J. (1998) Isolation and characterization of monomeric and dimeric CP47-reaction center photosystem II complexes, *J. Biol. Chem. 273*, 16122−16127.
67. Lyon, M. K. (1998) Multiple crystal types reveal photosystem II to be a dimer, *Biochim. Biophys. Acta 1364*, 403−419.

BI047685Q